

What Matters in Learning A Zero-Shot Sim-to-Real RL Policy for Quadrotor Control? A Comprehensive Study

Jiayu Chen^{1*}, Chao Yu^{1*✉}, Yuqing Xie¹, Feng Gao¹, Yinuo Chen¹, Shu'ang Yu^{1,2},
Wenhao Tang³, Shilong Ji¹, Mo Mu¹, Yi Wu¹, Huazhong Yang¹, Yu Wang^{1✉}

Abstract—Executing precise and agile flight maneuvers is critical for quadrotors in various applications. Traditional quadrotor control approaches are limited by their reliance on flat trajectories or time-consuming optimization, which restricts their flexibility. Recently, reinforcement learning (RL)-based policy has emerged as a promising alternative due to its ability to directly map observations to actions, reducing the need for detailed system knowledge and actuation constraints. However, a significant challenge remains in bridging the sim-to-real gap, where RL-based policies often experience instability when deployed in real world. In this paper, we investigate key factors for learning robust RL-based control policies that are capable of zero-shot deployment in real-world quadrotors. We identify five critical factors: (1) introducing velocity and rotation matrix into the actor input, (2) incorporating time vector into the critic input, (3) using regularization of difference between successive actions as a smoothness reward, (4) applying system identification with selective randomization, and (5) using large batch sizes during training. Building on these insights, we develop a PPO-based training framework named *SimpleFlight*, which integrates these five techniques. We validate *SimpleFlight*'s efficacy on Crazyflie quadrotor, demonstrating that it achieves more than a 50% reduction in trajectory tracking error compared to state-of-the-art RL baselines, and achieves 70% improvement over the traditional MPC. The policy derived by *SimpleFlight* consistently excels across both smooth polynomial trajectories and challenging infeasible zigzag trajectories on small thrust-to-weight quadrotors. In contrast, baseline methods struggle with fast or infeasible trajectories. To support further research and reproducibility, we integrate *SimpleFlight* into a GPU-based simulator Omnidrones and provide open-source code and model checkpoints. We hope *SimpleFlight* will offer valuable insights for advancing RL-based quadrotor control. For more details, visit our project website at <https://sites.google.com/view/simpleflight/>.

I. INTRODUCTION

Executing precise and agile flight maneuvers is crucial for unmanned aerial vehicles (UAVs), particularly quadrotors, in a variety of applications, including package delivery [1], search and rescue [2], and infrastructure inspection [3].

Traditional quadrotor control methods encompass both model-based and model-free approaches. While effective, these methods are typically limited by their reliance on flat trajectories that comply with actuation constraints [4], [5] or

on accurate system modeling and the performance of solvers handling nonconvex optimization problems [6], [7]. These limitations can restrict the flexibility and expressiveness of the control policy. Recently, reinforcement learning (RL) has emerged as a promising alternative for quadrotor control, offering greater flexibility and efficiency [8], [9]. RL-based policies can directly map observations to actions, reducing the need for actuation constraints or detailed knowledge of system dynamics [10]. This enables lower control latency and holds potential for improved performance in quadrotor control tasks.

A significant challenge in RL-based quadrotor control is the sim-to-real gap, where policies trained in simulation often exhibit instability when deployed in the real world without additional fine-tuning. While various RL-based approaches have been proposed, there is no unified consensus on the key factors that contribute to training robust, zero-shot deployable control policies [11], [12], [13], [14], [15], [16]. For instance, while reward functions are commonly designed to constrain control commands and improve smoothness, it remains unclear which specific reward component is essential to ensure valid control commands while effectively achieving task success. Similarly, domain randomization is widely employed to bridge the sim-to-real gap, but the extent to which it is necessary for effective quadrotor control remains unclear. Moreover, are there any other factors that influence the training of robust and stable RL-based control policies?

In this work, we investigate key factors essential for learning robust RL-based control policies capable of zero-shot deployment in the real world. We identify and summarize five critical factors of the entire training pipeline from the perspective of input space design, reward design, and training techniques. (1) introducing velocity and rotation matrix into actor's input, (2) incorporating time vector into critic's input, (3) using regularization of difference between successive actions as a smoothness reward, (4) applying system identification to several key parameters with selective randomization, and (5) utilizing a large batch size during training. The first two factors focus on input space design to enhance policy learning in simulation, while the third factor, reward design, and the last two, training techniques, work together to help bridge the sim-to-real gap. We further develop a training framework based on proximal policy optimization (PPO) that incorporates these five techniques, called *SimpleFlight*.

We conduct extensive real-world experiments on the open-source, open-hardware nano quadrotor Crazyflie 2.1 [17] to validate the effectiveness of *SimpleFlight*. The policy derived by *SimpleFlight* achieves over a 50% reduction in trajectory

* Equal Contribution.

✉ Corresponding Authors. {yuchao, yu-wang}@tsinghua.edu.cn

¹Tsinghua University, Beijing, 100084, China.

²Shanghai Artificial Intelligence Laboratory, Shanghai, 200030, China.

³Tsinghua Shenzhen International Graduate School, Shenzhen, 518055, China.

This research was supported by National Natural Science Foundation of China (No.62406159, 62325405), Postdoctoral Fellowship Program of CPSF under Grant Number (GZC20240830, 2024M761676), China Postdoctoral Science Special Foundation 2024T170496.

tracking error compared to state-of-the-art (SOTA) RL-based baselines and 70% improvement over the traditional baseline model predictive control (MPC), despite not involving any tailored algorithmic or network architecture design. This improvement is consistent across both smooth polynomial trajectories, such as figure-eight with varying velocities, and challenging infeasible trajectories with sharp changes in direction, such as random zigzags. Notably, the policy derived by SimpleFlight is the only one capable of successfully completing all benchmark trajectories among all RL-based policies. In contrast, other methods fail when faced with fast or infeasible trajectories that push the quadrotor to the limits of its system performance, especially on platforms with small thrust-to-weight ratios like Crazyflie.

Furthermore, we integrate SimpleFlight into a high-parallel GPU-based simulator Omnidrones [18], and we open-source the code, model checkpoints, and benchmark tasks to ensure reproducibility. We believe that SimpleFlight will provide valuable insights to guide future research in RL-based quadrotor control. Our contributions can be summarized as follows:

- We investigate several key learning factors and develop a PPO-based training framework, SimpleFlight, for learning RL-based zero-shot sim-to-real policies.
- We conduct extensive real-world experiments on the Crazyflie to demonstrate the effectiveness of SimpleFlight. The policy derived by SimpleFlight is the only one capable of successfully completing all benchmarking trajectories, including both smooth and infeasible trajectories.
- SimpleFlight reduces trajectory tracking error by over 50% compared to SOTA RL baselines and a 70% improvement over the traditional baseline MPC, despite not employing any tailored algorithmic or network architecture design.
- We integrate SimpleFlight into the high-parallel GPU-based simulator Omnidrones and open-source checkpoints to ensure reproducibility.

II. RELATED WORK

A. Quadrotor Control

Fast and accurate control of quadrotors has attracted significant attention, leading to the development of various control strategies. Traditional approaches for quadrotor flight typically fall into two categories: model-free methods, such as proportional-integral-derivative (PID) controllers [19], and model-based strategies, including MPC [7]. PID controllers are widely used due to their simplicity, but their performance degrades significantly in challenging scenarios. MPC, on the other hand, optimizes control inputs online over a finite time horizon while considering system dynamics and constraints. However, MPC heavily relies on an accurate model of the quadrotor. Furthermore, its computational intensity makes it impractical for resource-constrained platforms. These limitations have spurred growing interest in learning-based approaches, particularly RL, as a promising alternative for robust and flexible control.

RL has shown great potential in generating end-to-end control policies capable of generalizing across diverse and complex real-world scenarios without requiring detailed knowledge

of system dynamics. Existing studies have demonstrated the application of RL for controlling quadrotors to achieve tasks such as hovering stabilization under highly challenging conditions [8], minimum-time flight in cluttered environments [20], superhuman-level drone racing [21], and aggressive flight maneuvers [22]. These advancements underscore the promise of RL in deriving robust and adaptable quadrotor control policies.

In this paper, we choose precise trajectory tracking as a benchmark task to assess the effectiveness of RL-based control policies, as the ability to follow arbitrary trajectories is a foundational ability for quadrotors to execute complex tasks. To demonstrate the generalizability of the proposed key factors, we perform extensive real-world experiments on various trajectories with different speeds. These include smooth trajectories, such as figure-eight and random polynomial trials, and challenging infeasible trajectories with sharp changes in direction, such as pentagram and random zigzags.

B. Benchmark for RL-based Quadrotor Control

RL-based policies often necessitate extensive training in simulation due to the high cost of real-world experiments. The learned policies are expected to perform zero-shot transfer from simulation to the real world. This remains a significant challenge for RL, with strategies such as system identification (SysID) [23], domain randomization (DR) [24], and input abstraction [25] proposed to mitigate the transfer gap.

Despite significant advancements in RL-based control methods, the key factors essential for training robust, zero-shot deployable control policies remain unclear. A prior benchmark study explored different policy output configurations and demonstrated the effectiveness of computing collective thrust and body rates (CTBR) over alternatives like linear velocities and single-rotor thrusts, particularly for sim-to-real transfer [15]. In this paper, we also adopt CTBR as the policy output. Another benchmark study investigated policy input configurations and found that providing more input information does not necessarily enhance performance. Minimal configurations, comprising only relative position error, rotation matrix, and actions, were shown to enable robust flight policies [16]. In this paper, we also analyze input configurations and further find that replacing actions with linear velocity can accelerate training and improve tracking performance.

While prior work has benchmarked specific aspects, such as input and output configurations, a comprehensive investigation into the critical factors across the entire RL training pipeline remains lacking, such as reward design and the extent to which domain randomization should be applied. Our study addresses this gap by conducting the first extensive analysis of the key factors influencing the RL training pipeline to derive a zero-shot deployable policy. Moreover, previous benchmarks have typically focused on smooth polynomial trajectories, whereas we evaluate our findings across a range of smooth and challenging infeasible trajectories, ensuring the robustness and generalizability of the findings.

III. PRELIMINARY

A. Problem Formulation

We formulate the quadrotor control problem as a Markov Decision Process (MDP). The MDP is defined as $M = \langle$

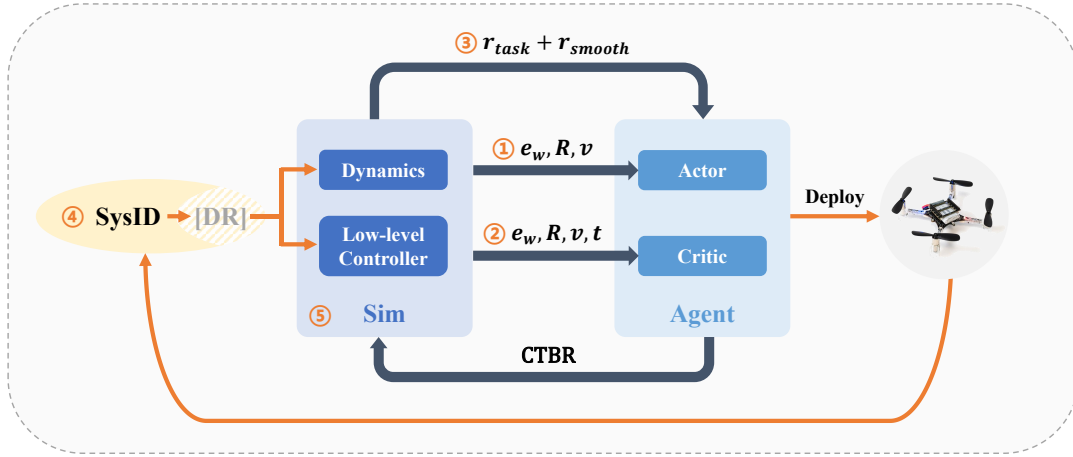


Fig. 1: Overview of SimpleFlight. We begin with SysID and selective DR for quadrotor dynamics and low-level control. Next, an RL policy is trained in simulation to output CTBR for tracking arbitrary trajectories and zero-shot deployed directly on a real quadrotor. The training framework focuses on three key aspects, i.e., input space design, reward design, and training techniques, identifying five critical factors to enhance zero-shot deployment.

$\mathcal{S}, \mathcal{A}, \mathcal{O}, \mathcal{P}, R, \gamma >$, with the state space \mathcal{S} , the action space \mathcal{A} , the observation space \mathcal{O} , the transition probability \mathcal{P} , the reward function \mathcal{R} and the discount factor γ . Denote the state and the observation at time step t as $(s_t, o_t) \in (\mathcal{S}, \mathcal{O})$. The goal of our work is to construct a policy π_θ parameterized by θ to output action $a_t \sim \pi_\theta(o_t)$ that performs precise and agile maneuvers to *track arbitrary trajectories*. The optimization objective is to maximize the expected accumulative reward $J(\theta) = \mathbb{E}[\sum_t \gamma^t R(s_t, a_t)]$.

B. Quadrotor Dynamics

The quadrotor is assumed to be a 6 degree-of-freedom rigid body of mass m and diagonal moment of inertia matrix $\mathbf{I} = \text{diag}(I_x, I_y, I_z)$. The state space is 17-dimensional and the dynamics of the quadrotor are modeled by the differential equation:

$$\dot{\mathbf{x}} = \begin{bmatrix} \dot{\mathbf{p}}_{\mathcal{W}} \\ \dot{\mathbf{q}} \\ \dot{\mathbf{v}}_{\mathcal{W}} \\ \dot{\boldsymbol{\omega}}_{\mathcal{B}} \\ \dot{\boldsymbol{\Omega}} \end{bmatrix} = \begin{bmatrix} \mathbf{v}_{\mathcal{W}} \\ \mathbf{q} \otimes [0, \boldsymbol{\omega}_{\mathcal{B}}/2]^T \\ \frac{1}{m} \mathbf{q} \cdot \mathbf{f}_{prop} \cdot \bar{\mathbf{q}} + \mathbf{g}_{\mathcal{W}} \\ \mathbf{I}^{-1}(\boldsymbol{\tau}_{prop} - \boldsymbol{\omega}_{\mathcal{B}} \times (\mathbf{I}\boldsymbol{\omega}_{\mathcal{B}})) \\ T_m(\boldsymbol{\Omega}_{cmd} - \boldsymbol{\Omega}) \end{bmatrix}, \quad (1)$$

where the quadrotor state \mathbf{x} consists the position \mathbf{p} , the orientation \mathbf{q} in quaternions, the linear velocity \mathbf{v} , the angular velocity $\boldsymbol{\omega}$ and the rotational speed of the rotor $\boldsymbol{\Omega}$. m denotes mass. The subscripts \mathcal{W} and \mathcal{B} represent the world and body frame. The frame \mathcal{B} is located at the center of the mass of the quadrotor. The notation \otimes indicates the multiplication of two quaternions. $\bar{\mathbf{q}}$ is the quaternion's conjugate. $\mathbf{g}_{\mathcal{W}} = [0, 0, -9.81m/s^2]^T$ denotes earth's gravity. \mathbf{f}_{prop} and $\boldsymbol{\tau}_{prop}$ are the collective force and the torque produced by the propellers. The quantities are defined as follows,

$$\mathbf{f}_{prop} = \sum_i \mathbf{f}_j, \boldsymbol{\tau}_{prop} = \sum_j \boldsymbol{\tau}_j + \mathbf{r}_{p,j} \times \mathbf{f}_j, \quad (2)$$

where $\mathbf{r}_{p,j}$ is the location of propeller j expressed in the body frame, $\mathbf{f}_j, \boldsymbol{\tau}_j$ are the forces and torques generated by the j -th propeller. The rotational speeds of the four motors Ω_j are modeled as a first-order system with a time constant T_m , where

the commanded rotational speeds $\boldsymbol{\Omega}_{cmd}$ serve as the input. For the forces and torques generated by each motor, we adopt a widely used model from prior work [26], [27]:

$$\mathbf{f}_j = [0, 0, k_f \Omega_j^2]^T, \boldsymbol{\tau}_j = [0, 0, k_m \Omega_j^2]^T. \quad (3)$$

The thrust and torque are modeled as proportional to the square of the motor's rotational speed. The corresponding thrust and drag coefficients, k_f and k_m , as well as the motor time constant, T_m , can be determined using a static propeller test stand.

IV. SIMPLEFLIGHT

A. Overview

In this section, we describe the details of the entire training framework SimpleFlight, as shown in Fig. 1. The core idea of learning a zero-shot sim-to-real RL policy involves two main aspects: improving policy performance in simulation and bridging the sim-to-real gap to minimize performance drop when deploying the policy in the real world.

To this end, we follow standard practices by first performing SysID to bridge the sim-to-real gap. We calibrate the quadrotor's dynamics by estimating four key parameters: mass m , inertia matrix \mathbf{I} , thrust coefficient k_f , and motor time constant T_m . These calibrated parameters are then used to model the quadrotor in the simulation. Following previous work, we adopt CTBR as the policy action space, a mid-level control command that has been shown to be more robust to sim-to-real gap [15]. To convert CTBR commands into four motor thrusts, a low-level controller is employed. Furthermore, we align the low-level controller in the quadrotor firmware with the one used in the simulator by calibrating its system response, thereby further bridging the sim-to-real gap.

Next, we train an RL policy in a simulator to enable the quadrotor to track arbitrary trajectories, which is then directly deployed on a real quadrotor without fine-tuning. The training framework emphasizes three critical aspects to enhance zero-shot deployment performance: input space design, reward design, and training techniques. Specifically, input space design aims to improve policy performance in simulation, while reward

design and training techniques are tailored to reduce the sim-to-real gap. From these three aspects, we identify and summarize five critical factors. The final design of SimpleFlight is detailed in the following sections, while comparisons with alternative configurations are presented in the experiment section.

B. Input Space Design

We employ a custom asymmetric actor-critic architecture in SimpleFlight. The actor takes as input the relative positions of the quadrotor to the next N reference trajectory points in the world frame $e_{\mathcal{W}}$, the linear velocity v , and the rotation matrix R . This design allows the policy to perform long-horizon planning, which is particularly crucial for tracking infeasible trajectories with sharp turns. In practice, we set $N = 10$, with each point spaced by 0.05s. The critic, on the other hand, receives the same inputs as the actor, augmented with a time vector $\mathbf{f}_t = [t, \dots, t]^T \in \mathbb{R}^k$ as privileged information. The time vector is directly obtained by expanding the current timestep by k dimensions. The time vector enables the critic to capture temporal information, improving its ability to estimate state values effectively. Both the actor and critic use three-layer MLPs to encode their inputs into a latent vector, respectively. For the actor, this vector parameterizes a Gaussian distribution to generate CTBR actions. For the critic, the vector is further fed into an MLP to produce the estimated state value.

Factor 1: Utilizing the rotation matrix instead of a quaternion and incorporating linear velocity into the actor’s input.

Factor 2: Adding a time vector to the critic’s input to enhance its temporal awareness.

C. Reward Design

In simulation, RL policies often explore aggressive actions to optimize task performance. For instance, a policy might produce a collective thrust command that abruptly changes from maximum thrust at one timestep to 0 at the next. While such actions may execute without immediate instability in simulation, due to the sim-to-real gap, they become physically infeasible for real quadrotors and can lead to unstable behavior during deployment.

To address this, RL leverages reward design to regularize policy outputs. Existing studies incorporate auxiliary reward components to encourage smooth actions. In general, the reward function is defined as:

$$r = r_{task} + \lambda r_{smooth}, \quad (4)$$

where r_{task} represents the task-specific reward, and r_{smooth} is a smoothness reward designed to promote smooth actions. λ is the coefficient of the smoothness reward. We normalize both r_{task} and r_{smooth} to the range $[0, 1]$, allowing λ to represent the relative weight of the smoothness reward compared to the task-specific reward.

It is important to note the trade-off between r_{task} and r_{smooth} . While r_{smooth} discourages aggressive actions and enforces smoother commands, it can also restrict the quadrotor’s ability to exploit agile maneuvers essential for tackling complex and challenging tasks. In SimpleFlight, we adopt the form $\|\mathbf{u}_t - \mathbf{u}_{t-1}\|_2$ as the smoothness reward, where \mathbf{u}_t represents the policy’s action, i.e., CTBR. We hypothesize that this design

penalizes abrupt changes in policy output, serving as a soft yet direct constraint. This approach achieves a better trade-off between task completeness and action smoothness, enabling both stable and agile flight.

Factor 3: Incorporating regularization of the difference between successive actions as the smoothness reward.

D. Training Techniques

We use OmniDrones [18], a GPU-accelerated, highly parallel drone simulator, to train the quadrotor control policy using on-policy algorithm PPO [28]. The simulator operates at an effective frequency of 100 Hz, with a simulation timestep of 0.01s. We highlight two often-overlooked training techniques that significantly impact policy performance. First, DR, a standard approach to enhance policy generalization, is commonly applied to quadrotor dynamics parameters. However, our findings reveal that DR is not universally beneficial. Policies trained with calibrated dynamics parameters via SysID, without DR, consistently outperform those trained with DR. This is because DR increases the policy search space and learning complexity, which can degrade both simulation and real-world performance when accurate calibration is possible. Nonetheless, for parameters that cannot be reliably calibrated, DR remains a valuable tool for improving generalization. Second, increasing the batch size during training improves real-world performance despite having limited impact on simulation results. This benefit possibly arises from the enhanced data diversity generated by larger batch sizes, which strengthens the policy’s generalization capacity.

Factor 4: Applying SysID for key dynamics parameters calibration and using DR selectively.

Factor 5: Leveraging larger batch sizes during training.

V. EXPERIMENT

In this section, we first outline the experimental setup, followed by a performance comparison across all methods. We then provide an in-depth analysis of the key factors in SimpleFlight and their influence on tracking accuracy.

A. Experiment Setup

1) **Benchmark Trajectories:** We adopt two types of trajectories as benchmark trajectories: **smooth trajectories** (figure-eight and polynomial) and **infeasible trajectories** (pentagram and zigzag). The figure-eight and pentagram trajectories are deterministic, while the polynomial and zigzag trajectories are randomly generated for each trial. All trajectories start from the origin $(0, 0)$ with a fixed z -axis height. Examples of benchmark trajectories are shown in Fig. 2.

a. Figure-Eight The figure-eight trajectory is a periodic smooth curve defined as $\mathbf{p}(t) = [\cos(2\pi t/T), \sin(4\pi t/T)/2, 1]$, where T represents the time required to complete one figure-eight lap. We test three velocities by varying T : 15.0s (Slow), 5.5s (Normal), and 3.5s (Fast), corresponding to maximum velocities of 0.6m/s, 1.6m/s, and 2.5m/s in the reference trajectories, respectively.

b. Polynomial The smooth polynomial trajectory consists of multiple randomly generated 5-degree polynomial segments. The duration of each segment is randomly selected between

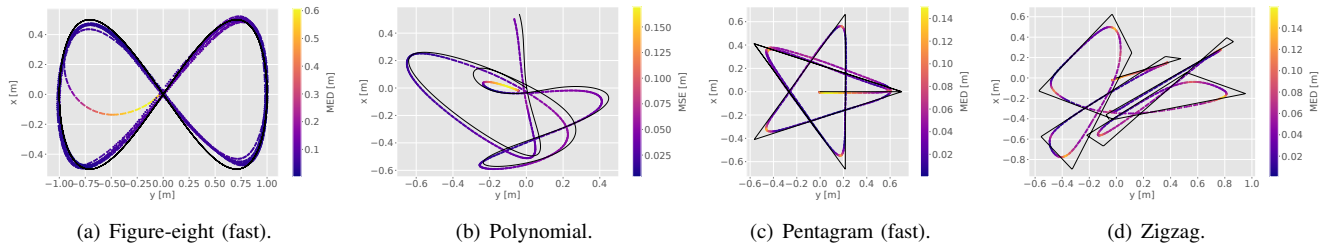


Fig. 2: Visualization of benchmark trajectories and corresponding trajectories followed using SimpleFlight. The reference trajectories are shown in black.

1.5s and 4s. The velocity of the reference trajectories ranges from 0 to 1m/s. To ensure smoothness, we enforce continuity of the first, second, and third derivatives at the junctions between consecutive segments.

c. Pentagon The pentagram is an infeasible trajectory where the quadrotor sequentially visits the five vertices of a pentagram at a constant velocity. We test two different velocities: 0.5m/s and 1m/s, marked as Slow and Fast, respectively.

d. Zigzag The zigzag trajectory is infeasible and is generated based on several randomly selected waypoints, with x - and y - coordinates distributed between -1 m and 1 m. Consecutive waypoints are connected by straight lines, with time intervals randomly chosen between 1s and 1.5s. The velocity of the reference trajectories ranges from 0 to 1m/s.

We note that pentagram and zigzag trajectories are challenging infeasible due to their sharp directional changes, i.e., infinite acceleration. Successfully tracking these trajectories requires quadrotors to perform long-horizon optimization and operate near the limits of their system performance, which is especially difficult for quadrotors with low thrust-to-weight ratios.

2) **Training and Deployment Details:** Training is performed on a diverse set of reference trajectories, including smooth randomized 5-degree polynomials and infeasible zigzag trajectories, which may have either zero or undefined accelerations. The policy is trained for 15,000 epochs and takes about 6 hours on an NVIDIA 4090 GPU. Note that we only derive one policy for all trajectories.

We deploy the derived policy on the open-source, open-hardware nano quadrotor Crazyflie 2.1. The position, velocity, and orientation are provided by an OptiTrack motion capture system at 100 Hz to an offboard computer that executes the policy. The CTBR control commands are transmitted to the quadrotor at 100 Hz via a 2.4 GHz radio. Note that although training is conducted using three random seeds, for deployment, we randomly select one policy rather than the best-performing one, as the training process demonstrates sufficient robustness.

3) **Baselines:** Although the primary goal of our paper is to investigate the key factors that enable robust RL-based control policies for zero-shot deployment in the real world (i.e., relative performance improvements), we also demonstrate the surprising effectiveness of SimpleFlight in terms of absolute performance. To this end, we reproduce two SOTA RL-based quadrotor control policies deployed on the Crazyflie as baselines, DATT [11] and Fly [14], as well as one traditional model-based baseline MPC [7].

a. DATT [11] is a novel feedforward-feedback-adaptive policy that outputs CTBR commands for tracking arbitrary trajectories. It achieves SOTA tracking performance, outperforming traditional controllers such as PID and MPC. Although DATT provides an open-source checkpoint, the quadrotor used in the original paper is a Crazyflie 2.1 with upgraded motors, offering a higher thrust-to-weight ratio. To ensure a fair comparison, we retrain DATT to match the Crazyflie 2.1 configuration used in this paper, specifically limiting the body rate to $[-\pi, \pi]$ rad/s and the acceleration to $[0, 1.6g]$, while keeping other settings unchanged. We deploy the DATT policy in the same way as SimpleFlight. Note that the disturbance estimation in DATT remains active in our experiments since it has better performance as reported in the original paper.

b. Fly [14] develops a high-speed simulator and proposes a training framework that enables sim-to-real transfer for direct Revolutions Per Minute (RPM) control. Fly trains an RL-based position controller in simulation, achieving superior zero-shot performance compared to both PID controller and prior RL-based policies in tracking figure-eight trajectories at various velocities on the real Crazyflie 2.1. In our experiments, we directly adopt the released checkpoint and performed onboard inference to track the benchmark trajectories.

c. MPC [7]. We employ Model Predictive Path Integral (MPPI), a sampling-based MPC approach that computes optimal actions by evaluating and weighting multiple candidate trajectories according to a defined cost function. We carefully fine-tune its parameters to ensure robust performance across all benchmark trajectories.

4) **Evaluation Metric:** We evaluate tracking performance by calculating the Mean Euclidean Distance (MED) between the quadrotor’s actual positions and the target position in the x - and y - axes, averaged over the entire trajectory. For the figure-eight trajectory, the quadrotor repeats the trajectory ten times per trial, and the MED is averaged across three trials. For the pentagram trajectory, the quadrotor completes the trajectory once per trial, and the MED is computed over three trials. For the polynomial and zigzag trajectories, we randomly generate five trajectories of each type, with each trajectory repeated twice, resulting in a total of ten trials. The MED is averaged over these ten trials. The numbers in all tables are presented in the format “mean (standard deviation)” with all values expressed in meters (m).

B. Main Results

We first report the trajectory tracking performance of SimpleFlight compared to the baseline methods across all

Methods	Figure-eight			Polynomial	Pentagram		Zigzag
	Slow	Normal	Fast		Slow	Fast	
MPC [29]	0.133(0.014)	0.205(0.018)	0.628(0.072)	0.206(0.037)	0.087(0.007)	0.159(0.004)	0.187(0.017)*
Fly [14]	0.093(0.001)	0.181(0.004)	0.282(0.012)	0.289(0.042)	0.104(0.005)	∞	∞
DATT [11]	0.050(0.009)	∞	∞	0.081(0.019)	0.055(0.004)	0.146(0.012)	0.114(0.019)*
SimpleFlight (Ours)	0.016(0.002)	0.028(0.000)	0.051(0.002)	0.032(0.003)	0.024(0.001)	0.045(0.002)	0.052(0.003)

TABLE I: Real-world Trajectory tracking performance comparison of all methods across benchmark trajectories. SimpleFlight achieves significantly better results than all baseline methods, reducing MED by over 50% on average. Notably, SimpleFlight is the only method capable of successfully completing both smooth and complex infeasible trajectories, demonstrating robust and accurate tracking across arbitrary trajectories. * indicates that for MPC and DATT in the zigzag trajectory trials, 4 out of 10 attempts failed; the reported MED reflects the 4 successful trials.

benchmark trajectories, as shown in Tab. I. SimpleFlight outperforms all baseline methods by a substantial margin, reducing the MED by more than 50% compared to RL-based approaches and 70% improvement over the traditional MPC baseline. Notably, among RL-based approaches, SimpleFlight is the only one capable of completing both smooth and complex infeasible trajectories. Furthermore, it achieves the lowest standard deviation across all baselines, indicating highly stable tracking performance. Fly learns a reliable position controller that can track smooth trajectories at different velocities, but it performs with larger tracking errors and fails to track infeasible trajectories like the fast pentagram and zigzag. This is mainly due to its lack of long-horizon reasoning ability, which limits its performance on sharp turns and complex paths. DATT, on the other hand, learns an aggressive policy that can handle infeasible trajectories but struggles with high-velocity tracking when using a quadrotor with a small thrust-to-weight ratio. This reflects the superior control performance of SimpleFlight, which excels in awareness of actuation constraints, long-horizon reasoning, and optimization, especially when facing sharp turns and complex maneuvers.

We remark that the comparison in Tab. I may not be entirely fair, as the policies are trained using different simulators, modeling approaches, and inputs/outputs. What we aim to convey here is that SimpleFlight, to the best of our knowledge, achieves the best control performance, despite not incorporating any algorithmic or architectural improvements. As a collection of proposed key factors, SimpleFlight can be integrated on top of existing quadrotor control methods.

We also conduct experiments on a self-built, larger quadrotor equipped with an Nvidia Orin processor to validate the effectiveness of SimpleFlight. Due to space constraints, the results of the real-world tracking experiments and accompanying video can be found on our website.

C. In-depth Analysis on Key Factors

In this section, we conduct ablation studies to evaluate the impact of the proposed key factors. Both simulation and real-world evaluations are conducted on figure-eight trajectories.

1) **Factors 1&2: Input Space Design:** Fig. 3 illustrates the training curves for different input space designs. For the actor (Fig. 3(a)), \mathbf{q} denotes the quaternion corresponding to the rotation matrix \mathbf{R} . Leveraging the relative positions $e_{\mathcal{V}\mathcal{V}}$, linear velocity \mathbf{v} , and the rotation matrix \mathbf{R} achieves the

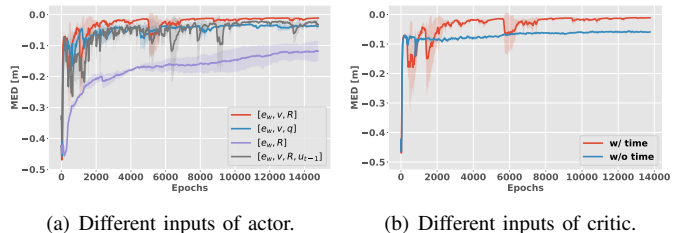


Fig. 3: Training curves of different input space designs. For the actor, the input comprising the relative positions $e_{\mathcal{V}\mathcal{V}}$, linear velocity \mathbf{v} , and the rotation matrix \mathbf{R} achieves the lowest MED in simulation. For the critic, incorporating time vector significantly enhances tracking performance.

best tracking performance in simulation. We observe a slight performance degradation when replacing \mathbf{R} with \mathbf{q} . This is because representations for the 3D rotations are discontinuous in four or fewer dimensions, making it challenging for neural networks to learn, as also observed in graphics and vision studies [30]. Excluding the linear velocity \mathbf{v} significantly degrades performance, underscoring its importance for predicting actions in agile quadrotor control. Including the previous action \mathbf{u}_{t-1} , as suggested in prior works [21], [16], results in a slight performance drop. We hypothesize that this is because the other inputs already provide sufficient information for tracking reference points. For the critic (Fig. 3(b)), incorporating a time vector greatly enhances tracking accuracy, demonstrating its utility in enabling the critic to better capture temporal information and estimate state values more effectively.

2) **Factor 3: Smoothness Reward Design:** We evaluate various smoothness components commonly used in existing studies, with the real-world tracking performance summarized in Tab. II. Here, $\text{acc}_t, \text{jerk}_t, \text{snap}_t$ represent the second, third, and fourth derivative of position at timestep t , respectively, and \mathbf{u}_t denotes the policy’s CTBR output at timestep t . Note that $\|\mathbf{u}_t\|_2$ penalizes desired angular velocity and thrust, indirectly constraining the third derivative of position, while $\|\mathbf{u}_t - \mathbf{u}_{t-1}\|_2$ penalizes angular acceleration and differential thrust, indirectly targeting the fourth derivative. The smoothness reward is defined as $r_{\text{aux}} = e^{-A}$, where A represents different forms of smoothness reward components. A grid search is conducted to optimize the hyperparameters for each component, and the best results are reported. In addition to reward design, we examine two alternative methods to encourage valid and smooth com-

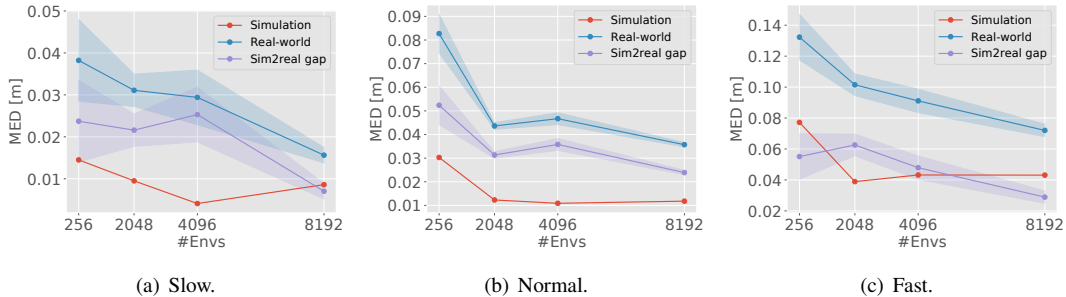


Fig. 4: The tracking performance of policies trained using different parallel environments. As the parallel environments increase, the tracking performance in perfect simulation remains similar. However, real-world performance improves, with the sim-to-real difference becoming smaller.

mands: “Action Clipping (AC)” and “Low-Pass Filter (LPF)”. AC directly limits actions exceeding a predefined threshold, while LPF smooths the policy output as $\mathbf{u}'_t = \alpha \mathbf{u}_t + (1 - \alpha) \mathbf{u}_{t-1}$, where α is the cutoff parameter. Among these, $\|\mathbf{u}_t - \mathbf{u}_{t-1}\|_2$ achieves the best real-world tracking performance. In contrast, non-reward methods like LPF fail to generalize across velocities, and AC limits agile maneuvers, resulting in suboptimal performance for high-velocity trajectories. Direct action constraints such as $\|\mathbf{u}_t\|_2$ outperform indirect kinematic constraints like $\|\mathbf{ jerk}_t\|_2$ on fast trajectories, highlighting the effectiveness of action-level regularization for challenging tasks.

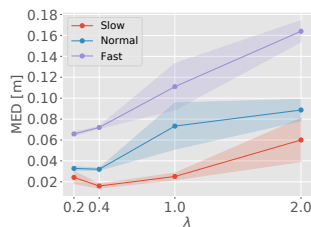


Fig. 5: Real-world performance of different λ on the figure-eight trajectory. We finally choose $\lambda = 0.4$.

	Slow	Normal	Fast
Action Clipping	0.035(0.001)	0.077(0.016)	0.310(0.016)
Low-Pass Filter	∞	∞	∞
$\ \mathbf{acc}_t\ _2$	0.183(0.004)	0.329(0.004)	∞
$\ \mathbf{ jerk}_t\ _2$	0.024(0.009)	0.047(0.005)	∞
$\ \mathbf{snap}_t\ _2$	0.026(0.002)	∞	∞
$\ \mathbf{u}_t\ _2$	0.044(0.003)	0.066(0.002)	0.110(0.027)
$\ \mathbf{u}_t - \mathbf{u}_{t-1}\ _2$	0.016(0.002)	0.028(0.000)	0.051(0.002)

TABLE II: Real-world tracking performance of different smoothness components that encourage valid and smooth control commands. The action-level regularization $\|\mathbf{u}_t - \mathbf{u}_{t-1}\|_2$ achieves the best tracking performance among all designs.

Since there exists a trade-off between the task reward and the smoothness reward, we conduct experiments on the smoothness reward coefficient λ , with the real-world tracking performance shown in Fig. 5. For $\lambda = 0.2$, not all fast trajectory experiments are successful; only results from successful trials are reported. As observed, larger λ can degrade tracking performance due to restricted agility, while smaller λ may lead to unstable flight. Based on these findings, we set $\lambda = 0.4$ for a balanced trade-off.

3) **Factor 4: SysID and DR:** We analyze the effects of SysID and DR on tracking performance for figure-eight trajectories

at normal velocity in Tab. III. We begin by calibrating four key dynamic parameters—mass m , inertia \mathbf{I} , motor time constant T_m , and thrust coefficient k_f —and report results using these calibrated values as “SysID”. We then apply DR to each parameter, exploring two parameter randomization ranges: $[-10\%, +10\%]$ and $[-30\%, +30\%]$, denoted as “SysID+DR10%” and “SysID+DR30%,” respectively. Our findings indicate that applying DR to approximately well-calibrated parameters generally does not improve sim-to-real transfer performance as it may increase learning complexity. In addition, introducing DR leads to slightly higher standard deviations, indicating that it can induce more unstable behavior. To further simulate inaccurate calibration, we introduce a +30% offset to each dynamics parameter, referred to as “Offset+30%.” This significantly worsens tracking performance, especially when offsetting the mass and thrust coefficient, underscoring the importance of accurately calibrating these two parameters. We then apply DR to these offset values (termed “Offset+DR30%”) and observe a noticeable improvement in the shifted thrust coefficient’s performance, alongside comparable results for the other parameters. This finding indicates that DR can be beneficial when parameters are not accurately calibrated. In summary, we recommend calibrating key quadrotor dynamics parameters and then selectively applying DR to mitigate residual uncertainties.

4) **Factor 5: Scaling Law of Batch Sizes:** To evaluate the impact of the batch sizes, we test simulation and real-world performance using figure-eight trajectories at three velocities via varying parallel environments. As shown in Fig. 4, increasing the number of parallel environments leads to convergence in simulation performance, while real-world performance continues to improve and the sim-to-real gap decreases. Based on these findings, we recommend using larger batch sizes during training to enhance sim-to-real transfer.

VI. CONCLUSION

We propose **SimpleFlight**, an RL-based framework designed to enable robust zero-shot deployment of control policies for real-world quadrotors. By identifying and integrating five key factors: enhanced input design with velocity and rotation matrix, time vector for the critic, regularization of the difference between successive actions as a smoothness reward, selective domain randomization with proper system identification, and large batch sizes during training. SimpleFlight narrows the

	Offset+30%	Offset+DR30%	SysID+DR30%	SysID+DR10%	SysID
Mass m	∞	∞	0.066(0.007)	0.041(0.006)	
Inertia I	0.041(0.004)	0.046(0.002)	0.053(0.005)	0.036(0.001)	0.028(0.000)
Motor Time Constant T_m	0.036(0.002)	0.044(0.002)	0.057(0.012)	0.040(0.001)	
Thrust Coefficient k_f	0.107(0.013)	0.035(0.001)	0.050(0.005)	0.034(0.002)	

TABLE III: Real-world tracking performance of SysID and DR on the figure-eight trajectory at normal velocity. For parameters that SysID can approximate with reasonable accuracy, introducing DR may lead to performance degradation by increasing learning complexity. When parameters cannot be accurately calibrated, incorporating DR can help improve performance.

sim-to-real gap effectively. Experiments on the off-the-shelf Crazyflie quadrotor show over a 50% reduction in trajectory tracking error compared to state-of-the-art RL baselines, with SimpleFlight uniquely completing all benchmark trajectories. Our open-source implementation with OmniDrones, combined with publicly accessible hardware, ensures reproducibility and lays a foundation for advancing RL-based quadrotor control. In this study, the quadrotor’s position and velocity are obtained using a motion capture system, with a maximum velocity of 2.5m/s. Future work could investigate the impact of noise in state estimation and extend the study to high-speed, complex, and vision-based tasks.

REFERENCES

- [1] J. Grzybowski, K. Latos, and R. Czyba, “Low-cost autonomous uav-based solutions to package delivery logistics,” in *Advanced, Contemporary Control: Proceedings of KKA 2020—The 20th Polish Control Conference, Łódź, Poland, 2020*. Springer, 2020, pp. 500–507.
- [2] J. Scherer, S. Yahyanejad, S. Hayat, E. Yanmaz, T. Andre, A. Khan, V. Vukadinovic, C. Bettstetter, H. Hellwagner, and B. Rinner, “An autonomous multi-uav system for search and rescue,” in *Proceedings of the first workshop on micro aerial vehicle networks, systems, and applications for civilian use*, 2015, pp. 33–38.
- [3] J. Nikolic, M. Burri, J. Rehder, S. Leutenegger, C. Huerzeler, and R. Siegwart, “A uav system for inspection of industrial facilities,” in *2013 IEEE Aerospace Conference*. IEEE, 2013, pp. 1–8.
- [4] D. Mellinger and V. Kumar, “Minimum snap trajectory generation and control for quadrotors,” in *2011 IEEE International Conference on Robotics and Automation*, 2011, pp. 2520–2525.
- [5] M. Faessler, A. Franchi, and D. Scaramuzza, “Differential flatness of quadrotor dynamics subject to rotor drag for accurate tracking of high-speed trajectories,” *IEEE Robotics and Automation Letters*, vol. 3, no. 2, pp. 620–626, 2018.
- [6] D. Hanover, P. Foehn, S. Sun, E. Kaufmann, and D. Scaramuzza, “Performance, precision, and payloads: Adaptive nonlinear mpc for quadrotors,” *IEEE Robotics and Automation Letters*, vol. 7, no. 2, pp. 690–697, 2021.
- [7] G. Williams, N. Wagener, B. Goldfain, P. Drews, J. M. Reh, B. Boots, and E. A. Theodorou, “Information theoretic mpc for model-based reinforcement learning,” in *2017 IEEE International Conference on Robotics and Automation (ICRA)*, 2017, pp. 1714–1721.
- [8] J. Hwangbo, I. Sa, R. Siegwart, and M. Hutter, “Control of a quadrotor with reinforcement learning,” *IEEE Robotics and Automation Letters*, vol. 2, no. 4, pp. 2096–2103, 2017.
- [9] B. Kiumarsi, K. G. Vamvoudakis, H. Modares, and F. L. Lewis, “Optimal and autonomous control using reinforcement learning: A survey,” *IEEE transactions on neural networks and learning systems*, vol. 29, no. 6, pp. 2042–2062, 2017.
- [10] C. Pfeiffer, S. Wengeler, A. Loquercio, and D. Scaramuzza, “Visual attention prediction improves performance of autonomous drone racing agents,” *Plos one*, vol. 17, no. 3, p. e0264471, 2022.
- [11] K. Huang, R. Rana, A. Spitzer, G. Shi, and B. Boots, “Datt: Deep adaptive trajectory tracking for quadrotor control,” in *Conference on Robot Learning*. PMLR, 2023, pp. 326–340.
- [12] F. Gao, C. Yu, Y. Wang, and Y. Wu, “Neural internal model control: Learning a robust control policy via predictive error feedback,” *arXiv preprint arXiv: 2411.13079*, 2024.
- [13] Y. Song, M. Steinweg, E. Kaufmann, and D. Scaramuzza, “Autonomous drone racing with deep reinforcement learning,” in *2021 IEEE/RSJ International Conference on Intelligent Robots and Systems (IROS)*. IEEE, 2021, pp. 1205–1212.
- [14] J. Eschmann, D. Albani, and G. Loianno, “Learning to fly in seconds,” *IEEE Robotics and Automation Letters*, vol. 9, no. 7, pp. 6336–6343, 2024.
- [15] E. Kaufmann, L. Bauersfeld, and D. Scaramuzza, “A benchmark comparison of learned control policies for agile quadrotor flight,” in *2022 International Conference on Robotics and Automation (ICRA)*. IEEE, 2022, pp. 10 504–10 510.
- [16] A. Dionigi, G. Costante, and G. Loianno, “The power of input: Benchmarking zero-shot sim-to-real transfer of reinforcement learning control policies for quadrotor control,” 2024. [Online]. Available: <https://arxiv.org/abs/2410.07686>
- [17] Bitcraze. (2024) Crazyflie 2.1. Accessed: 2024-12-05. [Online]. Available: <https://www.bitcraze.io/products/old-products/crazyflie-2-1/>
- [18] B. Xu, F. Gao, C. Yu, R. Zhang, Y. Wu, and Y. Wang, “OmniDrones: An efficient and flexible platform for reinforcement learning in drone control,” *IEEE Robotics and Automation Letters*, 2024.
- [19] S. Bouabdallah, P. Murrieri, and R. Siegwart, “Design and control of an indoor micro quadrotor,” in *IEEE International Conference on Robotics and Automation, 2004. Proceedings. ICRA’04. 2004*, vol. 5. IEEE, 2004, pp. 4393–4398.
- [20] R. Penicka, Y. Song, E. Kaufmann, and D. Scaramuzza, “Learning minimum-time flight in cluttered environments,” *IEEE Robotics and Automation Letters*, vol. 7, no. 3, pp. 7209–7216, 2022.
- [21] E. Kaufmann, L. Bauersfeld, A. Loquercio, M. Müller, V. Koltun, and D. Scaramuzza, “Champion-level drone racing using deep reinforcement learning,” *Nature*, vol. 620, no. 7976, pp. 982–987, 2023.
- [22] Q. Sun, J. Fang, W. X. Zheng, and Y. Tang, “Aggressive quadrotor flight using curiosity-driven reinforcement learning,” *IEEE Transactions on Industrial Electronics*, vol. 69, no. 12, pp. 13 838–13 848, 2022.
- [23] L. Bauersfeld, E. Kaufmann, P. Foehn, S. Sun, and D. Scaramuzza, “Neurobem: Hybrid aerodynamic quadrotor model,” *arXiv preprint arXiv:2106.08015*, 2021.
- [24] A. Molchanov, T. Chen, W. Hönig, J. A. Preiss, N. Ayanian, and G. S. Sukhatme, “Sim-to-(multi)-real: Transfer of low-level robust control policies to multiple quadrotors,” in *2019 IEEE/RSJ International Conference on Intelligent Robots and Systems (IROS)*, 2019, pp. 59–66.
- [25] A. Loquercio, E. Kaufmann, R. Ranftl, M. Müller, V. Koltun, and D. Scaramuzza, “Learning high-speed flight in the wild,” *Science Robotics*, vol. 6, no. 59, p. eabg5810, 2021.
- [26] F. Furrer, M. Burri, M. Achtelik, and R. Siegwart, “Rotors—a modular gazebo mav simulator framework,” *Robot Operating System (ROS) The Complete Reference (Volume 1)*, pp. 595–625, 2016.
- [27] S. Shah, D. Dey, C. Lovett, and A. Kapoor, “Airsim: High-fidelity visual and physical simulation for autonomous vehicles,” in *Field and Service Robotics: Results of the 11th International Conference*. Springer, 2018, pp. 621–635.
- [28] J. Schulman, F. Wolski, P. Dhariwal, A. Radford, and O. Klimov, “Proximal policy optimization algorithms,” *arXiv preprint arXiv:1707.06347*, 2017.
- [29] G. Williams, N. Wagener, B. Goldfain, P. Drews, J. M. Reh, B. Boots, and E. A. Theodorou, “Information theoretic mpc for model-based reinforcement learning,” in *2017 IEEE international conference on robotics and automation (ICRA)*. IEEE, 2017, pp. 1714–1721.
- [30] Y. Zhou, C. Barnes, J. Lu, J. Yang, and H. Li, “On the continuity of rotation representations in neural networks,” in *2019 IEEE/CVF Conference on Computer Vision and Pattern Recognition (CVPR)*, 2019, pp. 5738–5746.